Raman spectroscopy study of the influence of processing conditions on the structure of polycrystalline diamond films

R. Ramamurti, V. Shanov, and R. N. Singh[a)]
Department of Chemical and Materials Engineering, University of Cincinnati, Cincinnati, Ohio 45221-0012

S. Mamedov and P. Boolchand
Department of Electrical and Computer Engineering and Computer Science, University of Cincinnati, Cincinnati, Ohio 45221-0030

(Received 17 May 2005; accepted 14 November 2005; published 8 February 2006)

Diamond films are prepared by microwave plasma-enhanced chemical-vapor deposition on Si (100) substrates using the $H_2-Ar-CH_4$ gases. Raman scattering data, including the peak position, intensity, area, and width, are analyzed in depth and used to obtain the sp^3- and sp^2-bonded carbon contents and the nature of internal stresses in the films. Polarization behavior of the Raman peaks is analyzed to assess its role on the quantitative analysis of the diamond films, which suggested that the 1150 cm^{-1} Raman peak in nanocrystalline diamond films could be attributed to sp^2-bonded carbon. The role of the H_2/Ar content in the gas mixture and substrate temperature on the characteristics of the diamond film is studied. Thickness and grain size of diamond films are also determined by scanning electron microscopy and related to the *deposition conditions* and Raman results. Deposition conditions, which led to *highest* sp^3-bonded carbon content *and* growth rate, are identified. © *2006 American Vacuum Society.* [DOI: 10.1116/1.2150228]

I. INTRODUCTION

Microwave plasma-enhanced chemical-vapor deposition (MPECVD) has been widely used for deposition of diamond thin films.[1–9] Typically, hydrogen-methane gas mixtures are used as precursors although other gases such as nitrogen and noble gases have also been used to grow smooth nanocrystalline films.[1] The demand for films with consistent grain size is obvious, especially when polycrystalline diamond (PCD) is considered for optical and electronic applications, because the related properties are affected by the grain size. To fabricate electronic and optical devices, smooth films are required, which can be obtained using nanometer-sized grains. Conventional CVD method of synthesizing diamond films relies on hydrocarbon precursors in the presence of a large excess of hydrogen.[2] Argon has been used in place of hydrogen in carbon-oxygen-argon or carbon-argon systems.[3,5] The addition of argon to the plasma leads to an increased plasma electron density that enhances ionization and dissociation associated with the plasma chemistry.[6,7] Growth theory for these plasma gases is different from the conventional type of gases. C_2 dimer seems to be the growth species for nanocrystalline diamond films as suggested by Gruen and co-workers.[1,3,8,9]

Raman scattering is a powerful tool to characterize structure and quality of carbon-based films. It permits to distinguish different bonding types, domain size, and internal stress.[10] The Raman mode line shape, mode centroid, mode full width at half maxima (FWHM), mode scattering strength, and mode polarization are some of the parameters that provide information on the structure of diamond films.[10] In the case of carbon films, an additional item of interest is whether atomic bonding in films is threefold coordinated (sp^2) as in graphite or fourfold coordinated (sp^3) as in diamond. Furthermore, films could be amorphous-crystalline-diamond like, and/or amorphous-crystalline-graphitic structures like.[11] The diamond Raman peak intensity should be proportional to the scattering cross section and concentration of the diamond. But the spectral response of the film shows complicated structure due to the luminescence and peak overlapping.[12] There are peaks located between diamond and graphite because of the graphitelike defects leading to mixed sp^3 and sp^2 bonding states.[12] In order to tailor the bonding state through process control, quantitative analysis of the bonding state and correlation among complementary methods is necessary.[13] Since the shape of Raman spectra of diamond films depends on the excitation wavelength, there is more than a little ambiguity in the determination of diamond and graphite concentration. Different authors also have pointed out difficulties encountered in the interpretation of Raman spectra of multicomponent carbonaceous films.[14–17]

In this article, we elucidate the role of deposition parameters, such as the effect of varying concentration of hydrogen and argon plasma gases, and the deposition temperature on the quality and grain size of the PCD. To determine the quality of the diamond films in terms of the sp^3/sp^2 content, Raman spectroscopy was used as a method for conducting this study. Scanning electron microscopy (SEM) was used to obtain the grain size, and optical emission spectroscopy (OES) during the deposition was used to identify the growth species.

[a)]Author to whom correspondence should be addressed; electronic mail: raj.singh@uc.edu

TABLE I. Summary of diamond film synthesized at 95 torr pressure, 900 W microwave power, and 5 h deposition time.

	Deposition parameters					
Sample ID	Temperature (°C)	Ar (SCCM)	H_2 (SCCM)	CH_4 (SCCM)	Thickness (μm)	Grain size (μm)
0A3	800	95	4	1	3.82	0.06
1A3	800	94	5	1		
2A3	800	90	9	1	6.58	0.12
3A3	800	80	19	1	6.87	1.26
4A3	800	60	39	1	6.8	2.24
5A3	800	40	59	1	4.3	1.44
6A3	800	20	79	1	2.74	1.20
7′A3	800	0	99	1	2.45	0.98
8A3	700	95	4	1	3.05	0.56
8′A3	900	95	4	1	2.8	0.6
9A3	600	95	4	1	2.29	0.59
9′A3	800	95	4	1	3.69	0.06
15A3	500	95	4	1	1.78	0.17

II. EXPERIMENTAL PROCEDURES

An electron cyclotron resonance MPECVD (ECR-MPECVD) reactor was used to deposit polycrystalline diamond films on silicon substrates. Further details on the MPECVD system can be found in our previous publications.[18,19] Silicon wafers, *p* type (100) diced into squares ($25\times25\times0.5$ mm^3), were used as substrates for deposition of PCD. Standard wafer cleaning and activation prior to deposition were used.[20–22] The substrate activation procedure included ultrasonic treatment with the slurry of 20–40 μm diamond grit for 2 h. This process was followed by rinsing in acetone and ethanol, and drying in a N_2 gas before placing into the reactor. Before deposition, a 30 min etching was done in the hydrogen plasma to remove the native oxide layer from the Si substrate. Mixtures of CH_4, Ar, and H_2 were used as the reactant gases. The flow rate of CH_4 was kept constant at 1 standard cubic centimeter in minute (SCCM) in all cases, while the flow rate of Ar was varied from 0 to 95 SCCM and supplemented by H_2 to maintain a 100 SCCM total flow rate. The deposition temperature in one set of experiments was fixed at 800 °C. The deposition time was maintained at 5 h. In another set of experiments the pressure, power, and gas flow rates (95 Ar, 1 CH_4, and 4 H_2 typical for nanocrystalline diamond synthesis) were kept constant and the temperature was varied from 500 to 900 °C. These deposition conditions are summarized in Table I.

A scanning electron microscope (SEM, Hitachi S4000) was used to examine the surface morphology of the samples. The growth rates were determined by measuring the film thickness using cross-sectional SEM and then dividing it by the deposition time. The grain size was measured by the line-intercept method of the SEM photos. Raman scattering utilized a model T 64000, Jobin Yvon triple monochromator system, equipped with an optical multichannel detector charge-coupled device (CCD) array with Olympus BX-41 microscope attachment.[23,24] The Raman scattering was performed using 514.5 nm wavelength from an Ar^+ ion laser. The 6–10 mW power was focused to a spot size of 2 μm diameter (objective of $\times80$) and spectra accumulated at room temperature. The resolution of the Raman system was 2.4 cm^{-1}. An Ocean Optics high-resolution HR2000CG-UV-NIR universal serial bus (USB) fiber optic spectrometer was used for the optical emission study of the plasma.

III. RAMAN VIBRATIONAL MODE ASSIGNMENTS

Raman spectroscopy is an excellent method for the characterization of diamond films. The success of Raman spectroscopy in CVD diamond characterization is based on the simple, fingerprintlike spectrum of genuine diamond that consists of only a single Raman line at 1332 cm^{-1} at room temperature.[25] Natural single-crystal graphite exhibits a single Raman, the so-called *G* peak at 1580 cm^{-1} that is associated with the carbon-carbon stretching mode. If the graphite becomes disordered within the carbon layers, the *G* peak broadens. For polycrystalline graphite, depending on the size of the crystallites, a second peak termed as *D* peak at 1357 cm^{-1} appears. If the long-range order of the crystalline material is lost, the carbon phase becomes glassy, *G* and *D* peaks broaden, and the *D* peak intensity increases and downshifts.[25] Additional peaks at 1200, 1300, and 1470 may also appear because of the amorphous carbon.[13] In addition, a rather broad Raman band around 1150 cm^{-1} has been attributed by some researchers to nanocrystalline diamond and by others to sp^2-bonded carbon.[26] A further contribution to the spectrum is due to the fluorescence, which yields a background of increasing intensity with increasing wave numbers.[27] The Raman spectra of nanocrystalline and microcrystalline diamond films can be deconvoluted into these peaks as shown in Figs. 1 and 2, respectively. The experimental Raman curve is fitted using these peaks by a PEAK FIT program to extract more scientific information from the individual peaks or bonding types in the diamond film. This is

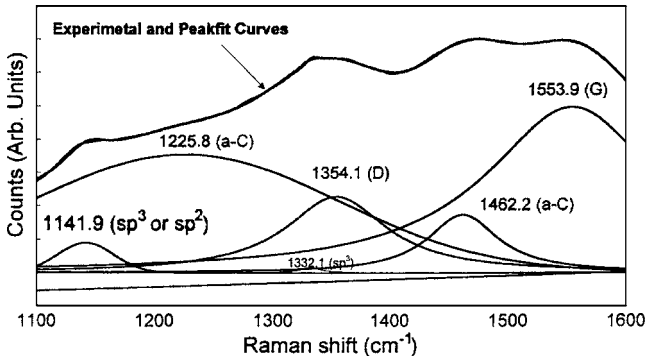

FIG. 1. Experimental and fitted spectra of a nanocrystalline diamond film and the deconvoluted spectra containing diamond and nondiamond contributing peaks.

done by performing line-shape analysis using the PEAK FIT software.[28] In this procedure, the linear background is subtracted and then peak characteristics are varied in an iterative manner to achieve an excellent agreement (high r^2 values) with the experimental data. Most of the fit displayed an r^2 value of 0.9998 with a 95% confidence limit. The r^2 value gives goodness of the fit and percentage confidence level indicates the level of confidence for the entire data set, including the value of intensity for a given value of the wave number. This numeric file from the PEAK FIT software gives information on the peak list, their fit type, peak intensity, width, and integrated area, which are then used to systematically study the effect of the processing variables on the properties of the diamond films synthesized in this study. The integrated areas were used in the evaluation of sp^3/sp^2 ratios using different approaches. Note that the Raman spectra become more complex for nanocrystalline diamond films because of the small grain size in comparison to the relatively large grained microcrystalline films. Table II gives the list of peak parameters that were used for quantitative analysis of this study. The Raman scattering cross sections for graphite *G* and *D* peaks relative to the characteristic diamond peak at 1332 cm^{-1} were experimentally measured by us for the Raman system using diamond and graphite standards and found to be 57 and 176 times larger than the diamond peak at the laser wavelength of 514.5 nm used in this study. A scattering cross section of 233 was assigned to amorphous carbon peaks at 1200, 1300, and 1470 cm^{-1} based on the published data.[29].

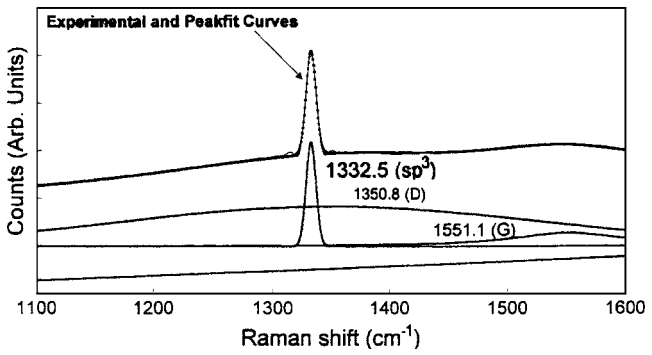

FIG. 2. Experimental and fitted spectra of a microcrystalline diamond film and the deconvoluted spectra containing diamond and nondiamond contributing peaks.

TABLE II. Summary of Raman mode assignments.

Nature of vibrations	Mode frequency (cm^{-1})	FWHM (cm^{-1})	Scattering cross section relative to the 1332 cm^{-1} mode	Depolarization ratio
sp^3 or sp^2[a]	~1150	80	1 or 57[b]	0.24
a-C[c]	1200	152	233[d]	0.24
a-C[c]	1300	132	233[d]	0.23
sp^3	1332	7	1	0.26
D[c]	1345	250	176	0.24
a-C[e]	~1470	80	233[d]	0.23
G[c]	1560	110	57	0.23

[a]Reference 31.
[b]Assigned a cross section of 1 if sp^3 bonded or 57 if sp^2 bonded.
[c]Reference 13.
[d]Reference 29.
[e]Reference 25.

IV. LINE-SHAPE ANALYSIS

The diamond peak at 1332 cm^{-1} is always fitted by a Lorentzian+Gaussian shape whose width can change over a range of 18 cm^{-1} and position up to 1338 cm^{-1}. The other peaks fit to a Gaussian.[14] The broadest peak at 3143 cm^{-1} (not shown in the data and figures) is because of the fluorescence. The weak Lorentzian peak at 520 cm^{-1} is due to silicon and the Lorentzian *D* peak at 1345 cm^{-1} is due to a disordered graphite phase. However, the graphite *G* peak at 1560 cm^{-1} is fitted by a Gaussian. The peaks at 1150 cm^{-1} (Lorentzian nanocrystalline diamond) and 1470 cm^{-1} (Gaussian amorphous carbon) are also necessary to fit the experimental curve.[25] Nemanich *et al.*[11] proposed that the small grain size of diamond would be expected to relax the $q=0$ selection rule and allow contribution of phonon modes with q not equal to zero to the spectrum. This has been supported by other researchers.[30,31] Phonon confinement allows the participation of phonons with a wave vector $q \sim 2\pi/d$, where d is the grain size. Grains of 5–100 nm would still favor modes close to the center of Brillouin zone than modes nearer the zone boundary where the vibrational density of states (VDOS) is maximum. Even if the grains were truly 1 nm or less, the VDOS has a maximum near 1260 cm^{-1}, but not at 1150 cm^{-1}, so a single peak at 1150 cm^{-1} would not be seen.[26] The much larger signal from the sp^2 graphitic sites than the sp^3 diamond regions proves that this may be due to the nondiamond phase in the rather wide grain boundaries.[26] The Raman spectra taken at various excitation laser energies show a dispersion of the 1150 cm^{-1} peak.[26] If this is not a density-of-states feature, then it would not change with excitation energy. When excited with a 244 nm laser the 1150 cm^{-1} is absent indicating that it is sp^2-bonded graphite, since the sp^3 sites have their highest scattering cross sections at these energies.[26] The peaks in the

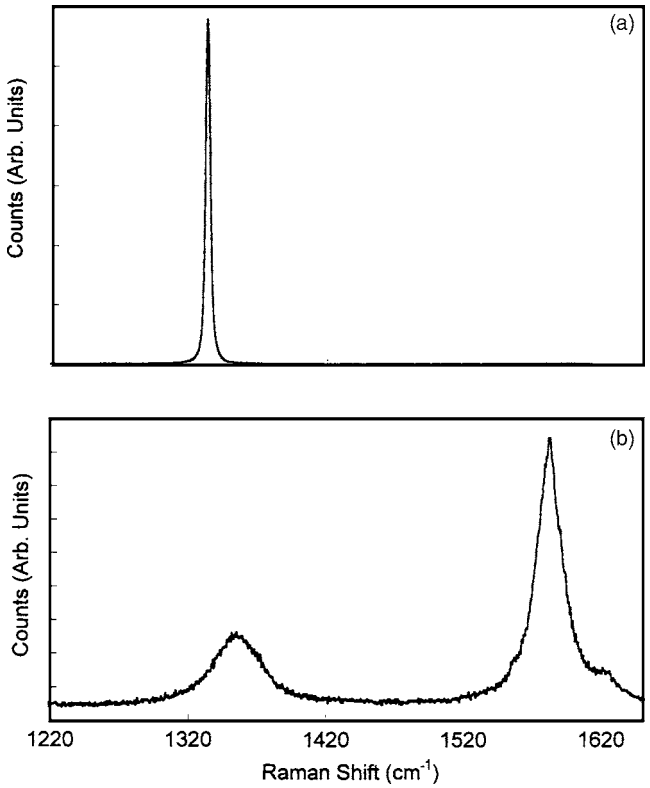

FIG. 3. Raman spectra from (a) pure diamond powder and (b) pure graphite powder of same amounts.

range of 1200–1300 cm^{-1} have been observed for "glassy carbon."[13] In order to determine the sp^3/sp^2 ratio, we have used the integrated areas of the diamond and graphite peaks with appropriate corrections for the measured areas based on all the scattering cross sections given in Table II. Throughout this article, we have used sp^3 mode as akin to diamond and sp^2 mode from *D* and *G* Raman peaks as graphite interchangeably.

Based on the above discussions, three approaches for evaluating diamond and graphite contents in the films were adopted. In each of these approaches, different ways of treating the 1150 cm^{-1} peak for calculation of the sp^3 to sp^2 ratios is utilized. (1) In the first approach, the 1150 and 1332 cm^{-1} peaks are chosen as diamond and the 1350 and 1560 cm^{-1} peaks are chosen as graphite. (2) In the second approach, the 1332 cm^{-1} peak is chosen as diamond and the 1150, 1350, and 1560 cm^{-1} peaks are chosen as graphite. (3) In the third approach, the 1150 cm^{-1} peak is taken as neither diamond nor graphite, the 1332 cm^{-1} peak is chosen as diamond, and the 1350 and 1560 cm^{-1} peaks are chosen as graphite. The 1200, 1300, and 1470 cm^{-1} peaks are chosen as amorphous carbon in the analysis. The area under the chosen peaks is used in the additive mode. The Raman spectra obtained from the 1 g of pure diamond (particle size of 20–40 μm) and1 g of pure graphite (particle size of 20 μm) powders as standards are shown in Figs. 3(a) and 3(b), respectively. These spectra were fitted to the appropriate peaks for calculating the scattering cross sections. The ratio of the integrated areas of 1332–1550 cm^{-1} was found to be 57. The ratio of the integrated areas of 1332–1350 cm^{-1} was found to be 176. The scattering cross section of 233 for amorphous carbon peaks (1460, 1200, and 1300 cm^{-1} peaks) was taken from previous studies.[29] Using appropriate scattering cross sections for the respective peaks, diamond and graphite contents can be given by the following equations.

Approach 1.

1150 cm^{-1}—considered as diamond,

$$R_{\text{diamond}} = (A_{1150} + A_{1332})/[A_{1332} + A_{1150} + A_{1550}/57 + A_{1350}/176 + (A_{1460} + A_{1200} + A_{1300})/233]$$

$$R_{\text{graphite}} = (A_{1550}/57 + A_{1350}/176)/[A_{1332} + A_{1150} + A_{1550}/57 + A_{1350}/176 + (A_{1460} + A_{1200} + A_{1300})/233].$$

Approach 2.

1150 cm^{-1}—considered as graphite,

$$R_{\text{diamond}} = A_{1332}/[A_{1332} + (A_{1150} + A_{1550})/57 + A_{1350}/176 + (A_{1460} + A_{1200} + A_{1300})/233]$$

$$R_{\text{graphite}} = [(A_{1150} + A_{1550})/57 + A_{1350}/176]/[A_{1332} + (A_{1150} + A_{1550})/57 + A_{1350}/176 + (A_{1460} + A_{1200} + A_{1300})/233].$$

Approach 3.

1150 cm^{-1}—considered as neither diamond nor graphite,

$$R_{\text{diamond}} = A_{1332}/[A_{1332} + A_{1550}/57 + A_{1350}/176 + (A_{1460} + A_{1200} + A_{1300})/233]$$

$$R_{\text{graphite}} = (A_{1550}/57 + A_{1350}/176)/[A_{1332} + A_{1550}/57 + A_{1350}/176 + (A_{1460} + A_{1200} + A_{1300})/233].$$

V. RESULTS AND DISCUSSION

Raman spectra for the diamond films grown at different H_2/Ar concentrations in the plasma are shown in Fig. 4. The sharpest Raman peak at 1332 cm^{-1} is seen for films grown at an intermediate (39% hydrogen) gas composition, and the quality of this peak significantly deteriorates at higher argon concentrations as evident from Fig. 4(b). These Raman data were analyzed using the three approaches described earlier in order to quantitatively assess the quality of diamond film in terms of the sp^3/sp^2 ratios. The calculated sp^3/sp^2 percentages with varying hydrogen/argon concentrations in the plasma are given in Figs. 5(a), 5(b), and 5(c) for approaches 1, 2, and 3, respectively. Note that the data in some of these figures do not add up to 100% because of the presence of *a*-carbon, which was included in the calculations but not in the plots. Generally, the increase of hydrogen in an argon plasma led to increased diamond (sp^3) content and decreased graphite (sp^2) content. The sample OA3 has the lowest sp^3 concentration and samples 3A3 and above has higher sp^3 concentration using approach 1. Similar trends are obtained using approaches 2 and 3 but the actual percentage of diamond and graphite can vary depending on the specific ap-

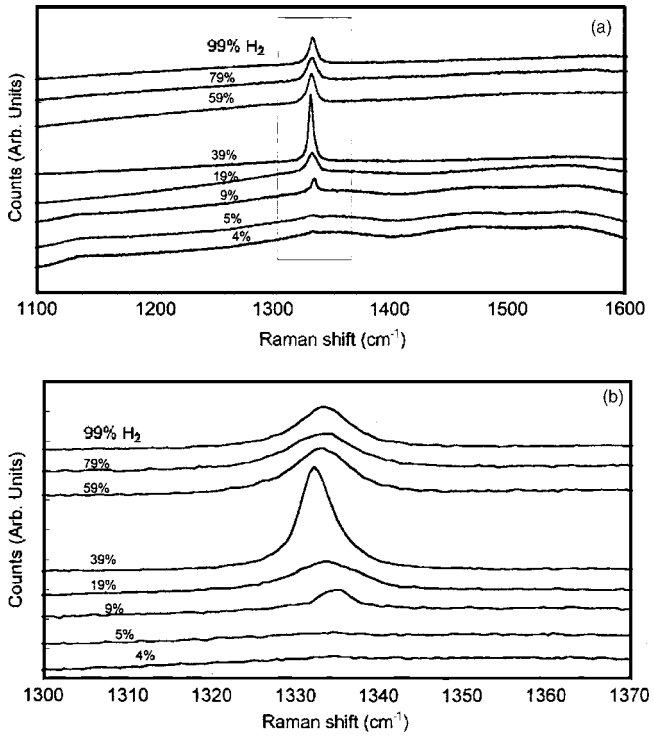

FIG. 4. (a) Raman spectra from diamond films grown under varying H_2/Ar concentrations, 1% CH_4, 95 torr, 800 °C, 900 W, 5 h, and (b) expanded view of the 1332 cm^{-1} sp^3 Raman mode.

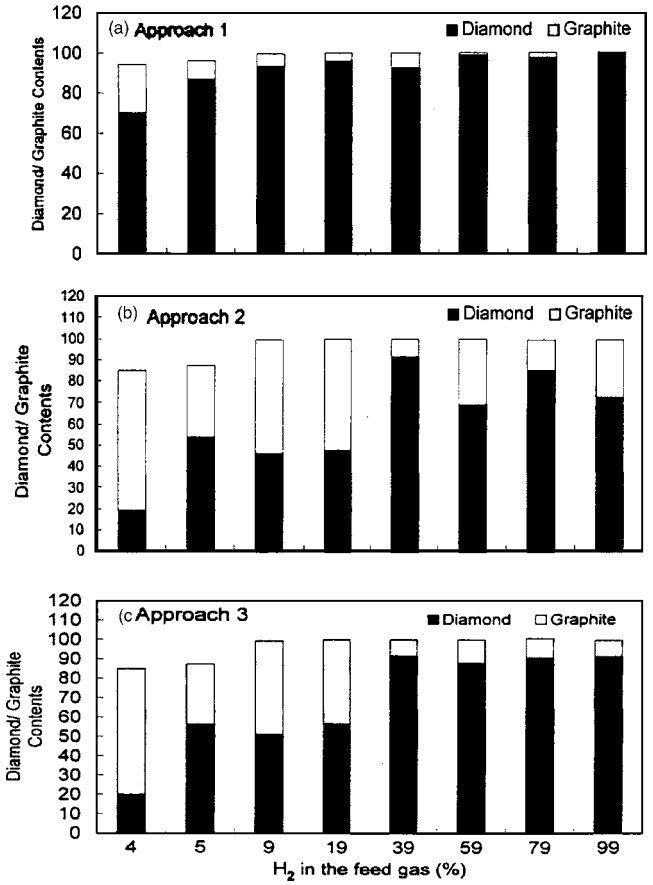

FIG. 5. Percentage sp^3/sp^2 contents in the diamond films deposited with varying H_2/Ar concentrations, 1% CH_4, 95 torr, 800 °C, 900 W, 5 h, using (a) approach 1, (b) approach 2, and (c) approach 3.

proach used to calculate the diamond content. It is also interesting to note that approach 1 gives the higher diamond content for all deposition parameters (Ar/H_2 ratio) because of the assumption that the 1150 cm^{-1} Raman peak is coming from the sp^3-bonded carbon. Much lower diamond contents are obtained in Fig. 5(b) using approach 2 because in this situation the 1150 cm^{-1} Raman peak is assumed to be from the sp^2-bonded carbon. Approach 3 gives intermediate values for the diamond content because of the total exclusion of the 1150 cm^{-1} Raman peak from the analyses. Approaches 2 and 3 give unusually low values of the diamond content ($\sim$20%) for extremely Ar-rich deposition conditions in which nanocrystalline diamond is formed. In fact, a significant variability in the diamond content is seen for plasmas containing less than $\sim$40% H_2 suggesting that Raman analysis may underestimate diamond content in situations where the grain size of the diamond is very small. However, a simple estimation based on the grain-boundary volume *assuming spherical grains* shows that the numbers calculated using Raman data are reasonable (as discussed later). However, other complementary techniques such as high-resolution transmission electron microscopy (HRTEM), electron-energy-loss spectroscopy (EELS), and near-edge x-ray-absorption fine structure (NEXAFS) may provide additional useful information on the quality of diamond films with very small grain size in the nanometer range.[32]

Diamond films synthesized in 39% H_2 and 60% Ar plasma composition show $\sim$93% diamond and 7% graphite irrespective of the quantification approaches used. In fact, the diamond peak at 1332 cm^{-1} shows an unusually sharp character even when compared to films grown in 99% H_2 plasma. This observation is quite interesting and may have implications on the microstructural features of the films as discussed later. These data clearly indicate that different quantitative results can be obtained depending on the type of analysis used to assess diamond quality using the Raman data. However, the qualitative trends on the effect of Ar/H_2 gas content on diamond quality remain unchanged irrespective of the type of analysis used to analyze the Raman data.

These results also agree with the theoretical understanding that secondary nucleation takes place when diamond is grown in plasmas containing high argon concentrations. This promotes growth of nondiamond phase at the grain boundaries due to increased C_2 dimer species in the plasma and causes the growth of nanocrystalline diamond.[1,8] In this mechanism, one C_2 adds to the surface by inserting itself into first one C–H bond and then a second C–H bond producing an adsorbed ethylenelike structure. A second C_2 then inserts itself into two adjacent C–H bonds to produce a surface with two adjacent ethylenelike groups.[9,33] Unlike methane, a carbon dimer is a highly energetic molecule that can insert directly into carbon-carbon and carbon-hydrogen bonds without the intervention of atomic hydrogen, creating the potential for a straightforward process for continuing growth of the diamond lattice.[3] At lower argon concentrations, there

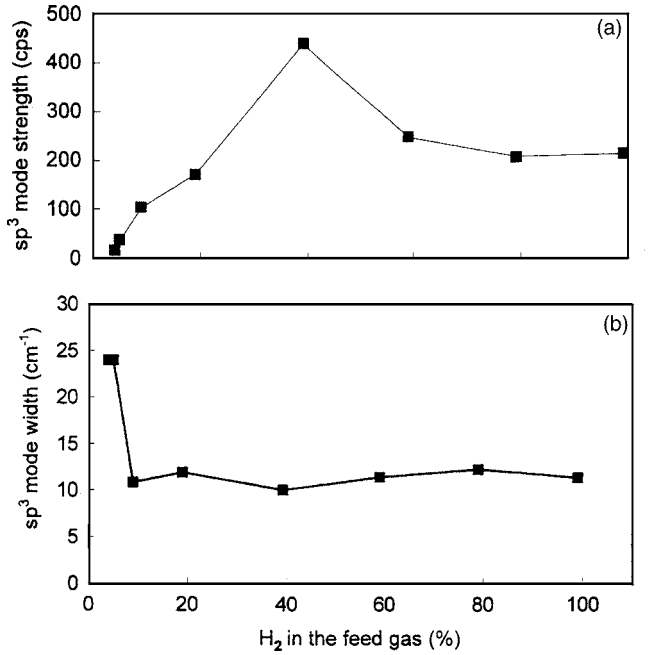

FIG. 6. Variations of (a) sp^3 mode scattering strength and (b) sp^3 mode width as a function of the hydrogen concentration in the feed gas.

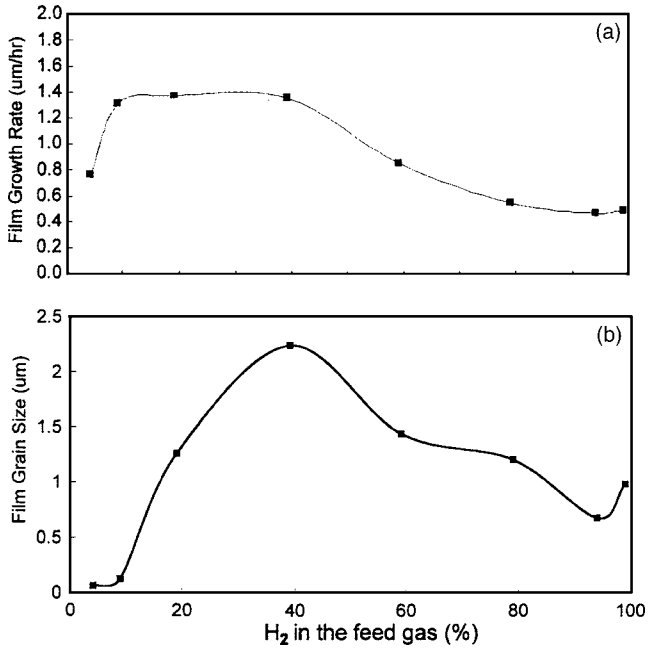

FIG. 7. Variation of (a) film growth rate and (b) film grain size with hydrogen concentration in the feed gas for films deposited at 800 °C using $Ar-H_2-CH_4$ gases.

is a lesser number of C_2 species and more CH_3 and CH species in the plasma, which suppresses secondary nucleation and promotes growth of the microcrystalline diamond.

The sp^3 content increases as the concentration of hydrogen in the plasma is increased from 5% to 99%. Further analysis of the diamond peak (1332 cm^{-1}) intensity and FWHM with hydrogen content is done and the results are shown in Figs. 6(a) and 6(b). The larger diamond peak intensity and smaller FWHM are consistent with the higher diamond content. Figure 6(a) reveals that the maximum diamond peak intensity is at 39% hydrogen and the corresponding FWHM is a minimum at this composition as seen in Fig. 6(b). This observation also indicates that best quality diamond film is synthesized at this intermediate H_2/Ar ratio in the plasma.

The growth rate and grain size of the diamond film are related to the film quality, i.e., it is generally understood that higher growth rates lead to smaller grain and lower quality diamond films. However, the experimental results from this study show somewhat different picture as given by the plot of growth rate and grain size versus hydrogen concentration in Fig. 7. The growth rates are highest over an optimum ratio of H_2/Ar in the plasma (20%–40%) and then drop off at very high and low ratios of the H_2/Ar in the plasma. The Raman results show that the films grown in plasma with 39% H_2 and 60% Ar produced the largest grain size (2.28 μm) and the highest growth rate (1.36 μm/h). These big grain size films show good quality diamond in terms of high intensity, sharp 1332 cm^{-1} Raman peak, and high purity. Change of the growth species from C_2 to CH_3 by increasing hydrogen concentration in argon plasma affects both the growth rate and the grain size of the PCD film. This transition takes place over a range of about 19%–39% H_2 content in the $Ar-H_2$ plasma as shown in Fig. 7. Consequently, the ability to deposit a desired diamond film (nanocrystalline versus microcrystalline) depends on the specific gas composition and other deposition parameters since the purity and overall quality of the diamond film are intimately related to processing.

The SEM of the diamond samples grown with 95%, 90%, 80%, and 60% argon are shown in Figs. 8(a)–8(d), respectively. The grain size of these films dramatically increases from 36 nm to 2.24 μm with decreasing argon content. Associated with increased grain size in Fig. 8(d) are also very clean and faceted grains grown using 60% argon. This again confirms that higher argon concentrations in the plasma of greater than 90% produces nanocrystalline diamond films as observed by other investigators.[1] The dominant growth species in the plasma can be determined by observing the optical emission spectra. As argon content is increased in the plasma from 60% to 95%, the C_2 peak intensities increased and reached a maximum at ~90% argon as illustrated in Figs. 9(a) and 9(b). This is also consistent with the fact that C_2 dimers, which promotes secondary nucleation, is the dominant growth species for nanocrystalline diamond films. In another study, the presence of sp^2-bonded phase at the grain boundaries in nanocrystalline films has been confirmed by Birrell *et al.*[34] using EELS measurements to compare the bonding structure in the diamond grains and the grain boundaries. The well-defined absorption edge at 289.5 eV in their results shows that the diamond grains are sp^3 bonded with high degree of short-range order. The grain-boundary spectra show the π^* peak at 285 eV, which is characteristic of nondiamond carbon phases.[34] These observations are also consistent with the quantitative data on diamond content in the films determined using Raman data in this study.

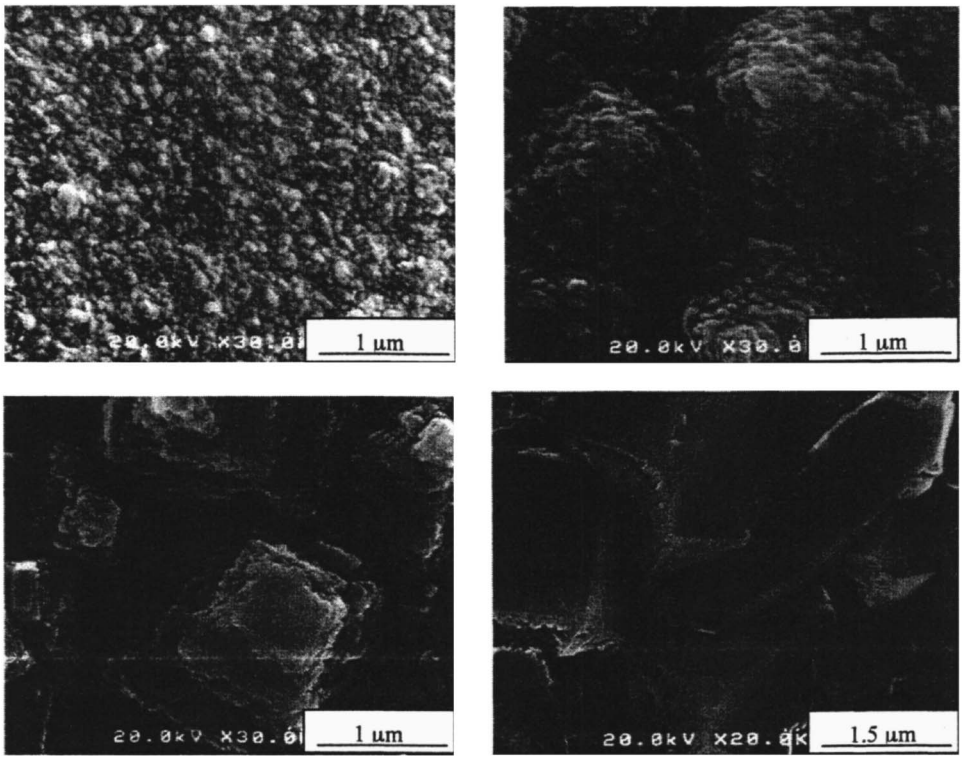

FIG. 8. SEM micrographs of diamond films showing the effect of gas composition on the growth morphology of films grown in (a) OA3 (95% Ar), (b) 2A3 (90% Ar), (c) 3A3 (80% Ar), and (d) 4A3 (60% Ar) (see Table I for more details).

A simple calculation of the sp^2 content in the films can be made using the grain size of the film relative to the grain-boundary thickness. The film grown at 95% Ar in the plasma produced nanocrystalline film with grain size of 60 nm. Assuming grain-boundary width of 1–3 nm (10–30 Å) gives the volume fraction of 10%–30% of the grain-boundary phase assuming spherical grains surrounded by grain boundary of a uniform thickness. If the grain boundaries are sp^2 bonded then these values of 10%–30% are not unreasonable for the sp^2 content in the diamond films. Significantly higher grain-boundary phase than this estimate is expected because of the grain intersections (triple points) of the polycrystalline nature of these films. We have ignored these in our simple-minded estimates. Consequently, nanocrystalline diamond films with very small grain size near 50 nm are expected to contain a significant proportion of the sp^2 or graphite phase at the grain boundaries and triple points as measured in this study using Raman spectroscopy. Recent estimates of 4%–10% sp^2-bonded carbon in ultrananocrystalline films are reported by Birrell *et al.* using NEXAFS.[32] While these films were synthesized using somewhat different plasma power and gases than used in our study, the accuracy of their estimation can be argued as mentioned by the authors themselves. However, there are no doubts that films with grains in the nanometer range are expected to contain a significant level of the nondiamond phase (other than the sp^3-bonded carbon) at the grain boundaries. Consequently, the results of this study are consistent with these observations.

The effect of substrate temperature on the sp^3/sp^2 content is also investigated by Raman technique for nanocrystalline films synthesized under the same ratios of the Ar/H_2 in the plasma, i.e., 95% Ar, 4% H_2, and 1% CH_4 to see if the films with an optimum diamond content can be synthesized. The Raman spectra for these films are shown in Fig. 10. The results of the quantitative analysis using Raman data are given in Figs. 11(a), 11(b), and 11(c) for approaches 1, 2, and 3, respectively. The diamond concentration changes as the temperature increases. At 600 °C the sp^3 content is maxi-

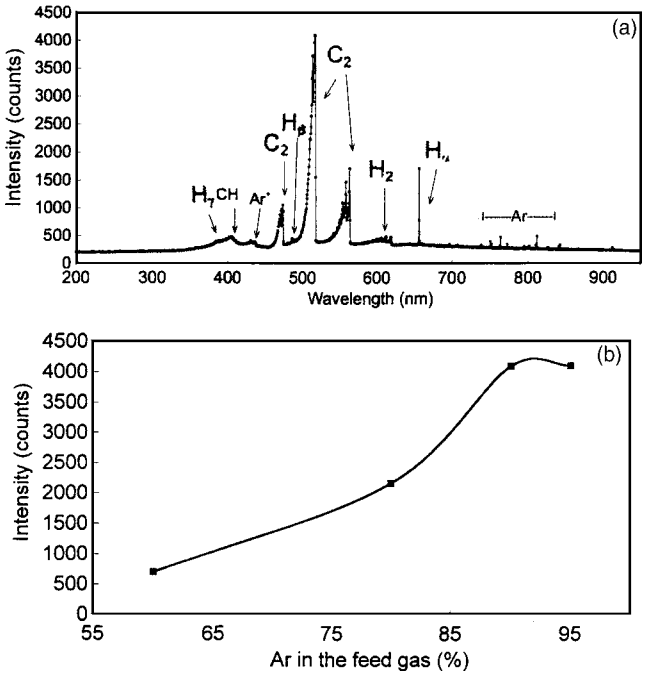

FIG. 9. Optical emission spectra from plasma of diamond film grown in 95% Ar, and (b) variation of C_2 intensity with Ar concentration in the feed gas.

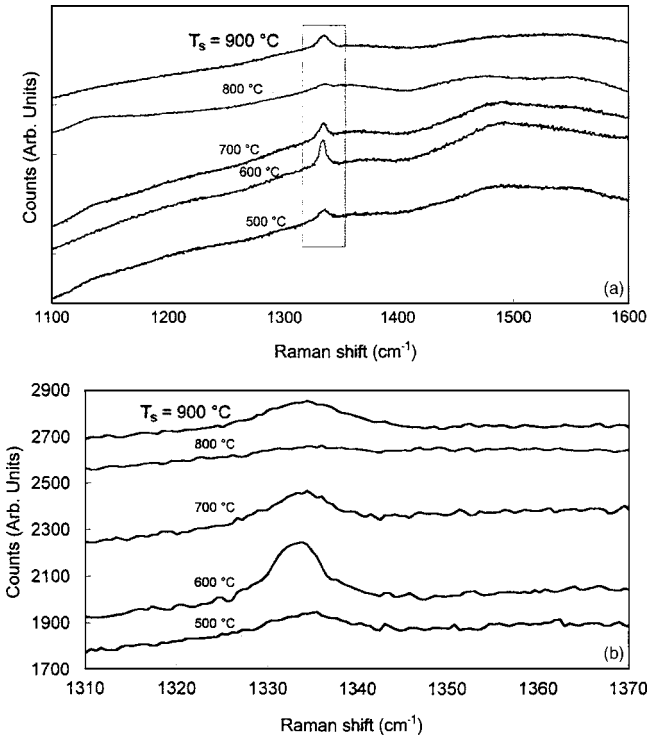

FIG. 10. (a) Raman spectra from diamond films grown under conditions of 95% Ar, 4% H_2, 1% CH_4, 95 torr, 900 W, and 5 h at different substrate temperatures. (b) Expanded view of the 1332 cm^{-1} sp^3 Raman mode.

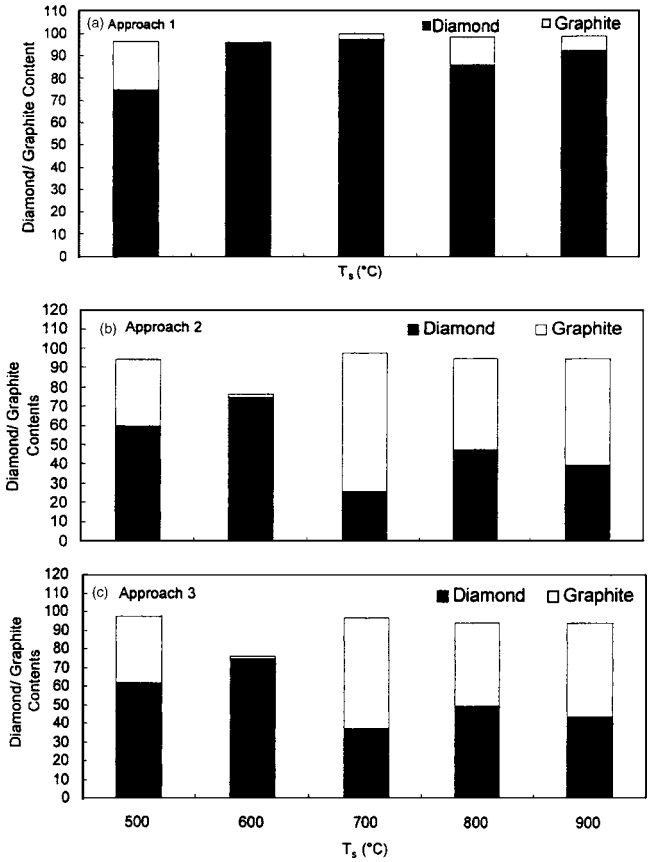

FIG. 11. Percentage of sp^3/sp^2 content in the diamond films deposited under conditions of 95% Ar, 4% H_2, 1% CH_4, 95 torr, 900 W, and 5 h as a function of varying substrate temperatures using (a) approach 1, (b) approach 2, and (c) approach 3.

mum and at 900 °C the amount of nondiamond phase is lower than at 500 °C using approach 1. Using approaches 2 and 3, the amount of nondiamond phase is higher at 900 °C than at 500 °C. These results suggest that the quality of the nanocrystalline diamond films can be enhanced by appropriate selection of the optimum deposition temperature.

Diamond films grown at substrate temperature (T_s) of 600 °C contains ~96% diamond and 0.29% graphite using approach 1 and 70.42%–76% sp^3-bonded carbon and 9.17%–1.67% sp^2-bonded carbon using approaches 2 and 3. In fact, films grown at 600 °C show highest diamond content by all approaches used. Amorphous carbon content is around ~5% for films grown at temperatures of 500, 700, and 800 °C using all approaches. The total peak height for the film grown at 600 °C is significantly below 100% because of the higher calculated *a*-C content of ~20%–25%. This requires further investigation to assess if the nanocrystalline films grown at 600 °C indeed contains a significant level of *a*-C. Approach 1 gives the highest concentration of sp^3 because of consideration of the 1150 cm^{-1}peak. Approach 2 shows lower sp^3 contents because 1150 cm^{-1} is considered sp^2. Approach 3 shows values of sp^3 between the above two approaches because 1150 cm^{-1} is neither sp^3 nor sp^2 bonded. These results indicate that the sp^3 content of the diamond film can be enhanced by deposition near 600 °C and Raman analysis of the data can be readily used for quantitative analysis of the films.

The variation of the diamond peak's (1332 cm^{-1}) intensity and FWHM with substrate temperature is shown in Figs. 12(a) and 12(b), respectively. It can be seen that the intensity is maximum near 600 to 700 °C. The corresponding FWHM plot shows a minimum at these temperatures. These results also suggest that temperature variations in the CVD process can affect the film quality. It impacts the reaction kinetics, especially for endothermic reactions such as methane decomposition, leading to a higher carbon flux in the gas phase at higher temperatures. This results in a higher supersaturation and hence higher chance for sp^2-bonded carbon formation in the film. At low substrate temperatures, the surface mobility of the carbon atoms is lower and hence the number of open sites for diamond formation is lower. This can result in the formation of more nondiamond phases. The films grown under the conditions of 95% Ar and 4% H_2 and 600 °C is expected to provide a better quality of nanocrystalline diamond compared to those grown at higher temperatures based on the results of this study. Therefore, optimum deposition temperature is also very important for synthesizing good quality nanocrystalline and microcrystalline diamond films.

The polarization of Raman peaks can also affect the quantitative assessment of film quality because it can influence the peak character. Consequently, the effect of polarization was studied. The polarization Raman studies gives information on the anisotropy in the films and enables calculation of depolarization ratio for different Raman scattering modes.

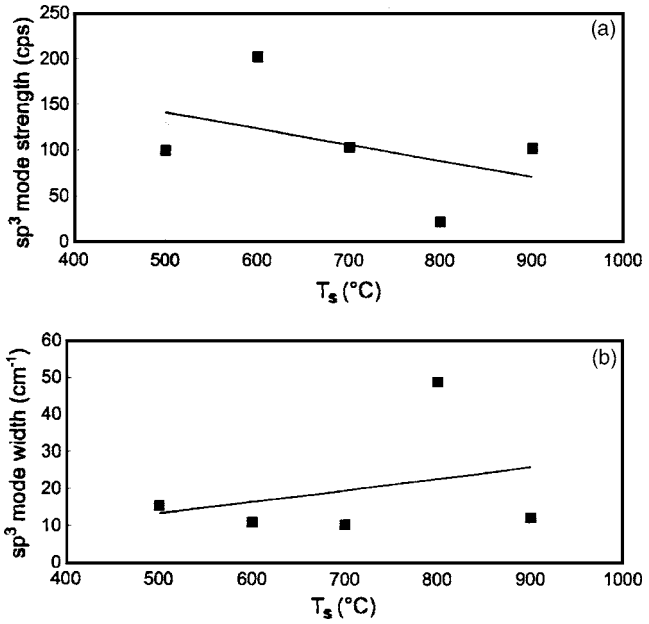

FIG. 12. Variation of (a) sp^3 mode scattering strength and (b) sp^3 mode width as a function of the substrate temperature.

The scattering process in a backscattering mode can be polarized in two ways: (1) vertical-vertical (VV), where the incident and scattered beams have the same polarization and (2) vertical-horizontal (VH), where the polarization of scattered beam is 90° to incident beam. The influence of the rotational, librational (rotation on small angle in solids), and vibrational motions on scattered spectrum may be described in terms of polarized and depolarized Raman intensities, I_{VV} and I_{VH}, respectively. The scattering, which comes from such vibrational modes where no change in form but only change in volume occurs, is called isotropic scattering.[35] The depolarized part of scattering, I_{VH}, comes from anisotropy of the polarizability tensor, in terms of whether the reason for anisotropy is rotation or libration of molecules (groups). The isotropic part just extracts "pure vibrations" from total scattering. However, this is valid only for isotropic media. Crystals are not isotropic media. The question on how the polarization properties *change* when adding small crystals to the isotropic disordered media is still unanswered. The ratio of the VH polarization to the VV polarization is given by I_{VH}/I_{VV}, which is called the depolarization ratio. This indicates if there is any particular mode that is strongly polarized.

The results of such polarization calculations are plotted for sample 2A3 (nanocrystalline diamond) in Fig. 13. It is found that the depolarization ratio for all the modes is a constant, in the range of 0.23–0.24, except for the 1332 cm^{-1} mode as given in Table II. This diamond peak has a depolarization ratio of 0.26 for sample 2A3, which is a little higher than the other modes. This means that there is some anisotropy in the films originating from the nature of crystal growth. Since the diamond 1332 cm^{-1} mode is polarized and the rest are not, there is an indication that the other modes should have nondiamond form. This also suggests the possibility that the 1150 cm^{-1} peak is not due to sp^3-bonded carbon. This is an additional rationale for assigning 1150 cm^{-1} Raman peak to sp^2-bonded carbon (graphite) in approach 2 of the peak fitting procedure used in this study. Using this rationale, it was possible to generate two more approaches (approaches 2 and 3) for using the Raman spectra for quantitative assessment of film quality in this study.

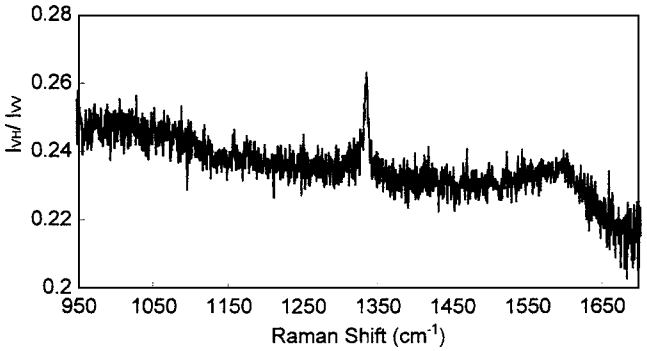

FIG. 13. Ratio of I_{VH}/I_{VV} polarizations for sample 2A3 deposited in 90% Ar in the feed gas.

Further analysis of the Raman data was done to see if the diamond peak positions have shifted systematically as a function of the deposition conditions. The resolution of the Raman system is 2.4 cm^{-1} and the data in Fig. 14 are obtained from PEAK FIT results rather than a casual look at the peak positions shown by the raw data in Fig. 4. The peak center for natural diamond is located at 1332.5 cm^{-1} and this is exactly where it is found for films grown with 39% H_2 in the Ar–H_2 plasma. However, the peak center is observed in this study to shift to a *higher wave number* at too low H_2 concentrations (<39%) in the plasma (indicating intrinsic

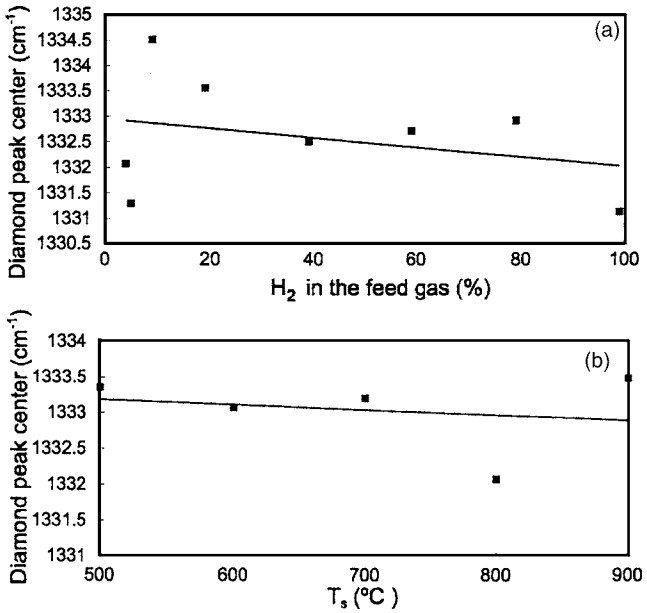

FIG. 14. Variation of diamond mode peak center with (a) hydrogen concentration in the plasma and deposited at 800 °C, and (b) substrate temperature for gas composition of 95% Ar, 4% H_2, and 1% CH_4. These data are from PEAK FIT analyses of the raw data in Fig. 4.

compressive stresses over a range of 0–1.5 GPa in the *nanocrystalline* films), and to a *lower wave number* at too high H_2 concentrations (>39%) (indicating a small tensile stress in the microcrystalline films) based on the least-squares line through the data in Fig. 14(a). It is interesting to note that films showing best quality in terms of the high sp^3 content and grown using ~39% H_2 are also close to being stress-free. Most of the nanocrystalline films grown using 4% H_2 and 95% Ar over the 500–900 °C temperature range show the peak center around 1333 cm^{-1} indicating *small* compressive residual stresses (except that grown at 800 °C where it is near 1332 cm^{-1}). Diamond films are expected to be generally in compression at room temperature based exclusively on the expansion mismatch between diamond and Si substrates (higher coefficient of expansion for Si than diamond). The majority of the observations on residual stresses are consistent with the expansion mismatch as being the dominant factor. However, the film thickness can also influence residual stresses but this was not controlled in this study and requires additional careful study to sort out the origin of residual stresses in films with different grain sizes.

VI. CONCLUSIONS

(1) Effects of the processing parameters such as flow rates of H_2, Ar, and CH_4 gases, temperature, and pressure on the synthesis of diamond films with a range of grain sizes from 60 nm to 2.2 μm were established.

(2) Effect of the processing conditions on the growth rates of the diamond films was studied. High growth rates of 1.4 μm/h was achieved for films processed at 800 °C using Ar(60%)–H_2(39%)–CH_4(1%) gas mixtures. Largest grain size was also obtained for films synthesized under these conditions. In contrast, films grown using Ar-rich gas mixtures (Ar-95%/H_2-4%/CH_4-1%) produced grains with 60 nm size.

(3) Quantitative measurements of the sp^3/sp^2 ratio in the CVD diamond films were done by Raman spectroscopy to assess their quality. Three different ways of analyzing Raman data were used depending on how to treat the 1150 cm^{-1} Raman peak seen in most nanocrystalline diamond films but not in microcrystalline films. The results indicated that higher hydrogen concentrations in the Ar–H_2 plasma increased both the sp^3 amount and the grain size. Quantitative analysis using the three approaches showed consistent results in terms of relative amounts of diamond and graphite. However, the results of this study indicated that the Raman peak at 1150 cm^{-1} cannot be considered as coming from sp^3-bonded carbon for estimating diamond quality in terms of the sp^3-bonded carbon. It is more reasonable to consider it coming from the sp^2-bonded carbon for estimating diamond quality, especially for nanocrystalline diamond films with very small grain size. The polarization Raman studies showed that the sp^3 mode located at 1332 cm^{-1} was polarized with a depolarization ratio of 0.26, which also suggested that the 1150 cm^{-1} Raman peak was not due to sp^3-bonded carbon. The best approach for estimating sp^3/sp^2content using Raman analyses of the diamond films was by treating the 1332 cm^{-1} peak as the sole contributor to the sp^3-bonded carbon and the 1150 cm^{-1} peak along with the *D* and *G* peaks as sp^2-bonded carbon.

(4) Diamond films grown with 60% Ar and 39% H_2 in the gas mixture displayed the best diamond quality (>90%) and had the highest growth rate and largest grain size. Those grown with 95% Ar and 4% H_2 had nanocrystalline grains and showed poor diamond quality (low sp^3 content of ~60%) based on this study. These results are reasonable because diamond films with grain sizes of ~60 nm are expected to contain a significant proportion (10%–30%) of the grain-boundary phase (non-sp^3 carbon or even amorphous carbon) as demonstrated by simple estimates based on typical thickness (1–3 nm) for the grain boundaries. Substrate temperature of 600 °C gave the best quality nanocrystalline diamond films with the highest sp^3 content (>75%) using some of the approaches of this study.

(5) The dominant growth species in Ar-rich Ar–H_2 plasma environment was identified as C_2 dimer. The intensity of C_2 species increased dramatically in plasmas containing 60%–95% argon, which had a dominant effect on the growth rate and grain size of the diamond films.

(6) The diamond film grown with 39% hydrogen in the Ar–H_2 gas mixture at 800 °C had the Raman peak center close to that of the stress-free natural diamond. Films grown with <39% H_2 in the plasma had slight compressive stresses. Nanocrystalline diamond films grown with 4% hydrogen–95% Ar displayed compressive stresses for depositions done over the temperature range of 500–900 °C. These results suggested that the origin of residual stresses in diamond films of this study was because of expansion mismatch between the Si substrate and diamond film.

ACKNOWLEDGMENTS

The authors thank Dr. Niloy Mukherjee at the Materials Science Characterization Center for help with the SEM and Dr. Daniel Georgiev for the Raman spectroscopy. The hints provided by Dr. Tao Qu and Dr. Fei Wang for using the PEAK FIT software have been very helpful. National Science Foundation under Grant Nos. ECS-0070004, CMS-0210351, and DMR-0200839 supported this project.

[1]D. Zhou, D. M. Gruen, L. C. Qin, T. G. McCauley, and A. R. Krauss, J. Appl. Phys. **84**, 1981 (1998).
[2]F. G. Celi and J. E. Butler, Annu. Rev. Phys. Chem. **42**, 643 (1991).
[3]D. M. Gruen, MRS Bull. **26**, 771 (2001).
[4]D. M. Gruen, S. Liu, A. R. Krauss, J. Luo, and X. Pan, Appl. Phys. Lett. **64**, 21 (1994).
[5]P. Joeris, C. Benndorf, and S. Bohr, J. Appl. Phys. **71**, 4638 (1992).
[6]H. C. Shih, C. P. Sung, W. L. Fan, and W. T. Hsu, Thin Solid Films **232**, 41 (1993).
[7]W. Zhu, A. Inspektor, A. R. Badzian, T. Mckenna, and R. Messier, J. Appl. Phys. **68**, 1489 (1990).
[8]D. M. Gruen, S. Liu, A. R. Krauss, J. Luo, and C. M. Foster, J. Vac. Sci. Technol. A **12**, 1491 (1994).
[9]P. C. Redfern, D. A. Horner, A. A. Curtiss, and D. M. Gruen, J. Phys. Chem. **100**, 654 (1996).

[10]P. R. Chalker, *Diamond and Diamond-Like Films and Coatings*, edited by R. E. Clausing, L. L. Horton, J. C. Angus, and P. Koidl (Plenum, New York, 1991), pp. 127–150.
[11]R. J. Nemanich, J. T. Glass, G. Lucovsky, and R. E. Shroder, J. Vac. Sci. Technol. A **6**, 1783 (1988).
[12]Y. V. Kaenel and J. S. E. Blank, Diamond Relat. Mater. **4**, 972 (1995).
[13]B. Marcus, L. Fayette, M. Mermoux, L. Abello, and G. Lucazeau, J. Appl. Phys. **76**, 3463 (1994).
[14]P. Bou and L. Vandenbulcke, J. Electrochem. Soc. **138**, 2991 (1991).
[15]V. Palshin, E. I. Meletis, S. Ves, and S. Logothetidis, Thin Solid Films **270**, 165 (1995).
[16]M. M. G. Poza, M. H. Velez, J. Jiminez, C. Gomez-Aleixandre, J. S. Olias, A. B. Montes, and J. M. Albella, Mater. Lett. **29**, 111 (1996).
[17]H. Chatei, J. Bougdira, M. Remy, P. Alnot, C. Bruch, and J. K. Kruger, Diamond Relat. Mater. **6**, 505 (1997).
[18]V. Shanov, W. Tabakoff, and R. N. Singh, J. Mater. Eng. Perform. **11**, 2 (2002).
[19]V. Shanov, R. N. Singh, and W. Tabakoff, *Proceedings of The International Conference on Metallurgical Coatings and Thin Films*, 10–14 April 2000, San Diego, California.
[20]R. Ramamurti, V. Shanov, R. N. Singh, M. Samiee, and P. Kosel, *Proceedings of The Sixth Applied Diamond Conference/Second Frontier Carbon Technology Joint Conference*, 4–10 August 2001, Auburn, Alabama, edited by Y. Tzeng, K. Miyoshi, M. Yoshikawa, M. Murakawa, Y. Koga, K. Kobashi, and G. A. J. Amaratunga (unpublished), pp. 64–67 (2001).
[21]M. Belmahi, F. Benedic, J. Bougdira, H. Chatei, M. Remy, and P. Alnot, Surf. Coat. Technol. **106**, 53 (1998).
[22]C. Sun, W. Zhang, C. Lee, I. Bello, and S. Lee, Diamond Relat. Mater. **8**, 1410 (1999).
[23]S. Mamedov, D. G. Georgiev, T. Qu, and P. Boolchand, J. Phys.: Condens. Matter **15**, S2397 (2003).
[24]X. Feng, W. J. Bresser, and P. Boolchand, Phys. Rev. Lett. **78**, 4422 (1997).
[25]P. K. Bachmann and D. U. Wiechert, *Diamond and Diamond-like Films and Coatings*, edited by R. E. Clausing, L. L. Horton, J. C. Angus, and P. Koidl (Plenum, New York, 1991), pp. 677–713.
[26]A. C. Ferrari and J. Robertson, Phys. Rev. B **63**, 121405 (2001).
[27]H. Chatei, J. Bougdira, M. Remy, P. Alnot, C. Bruch, and J. K. Kruger, Diamond Relat. Mater. **6**, 107 (1997).
[28]PEAK FIT 4.0 for Windows User's Manual, Peak Separation and Analysis Software, Copyright © 1997 by AISN Software, SPSS Inc., Chicago, IL, 1997.
[29]S. R. Sails, D. J. Gardiner, M. Bowden, J. Savage, and D. Rodway, Diamond Relat. Mater. **5**, 589 (1996).
[30]J. Wagner, M. Ramsteiner, C. Wild, and P. Koidl, Phys. Rev. B **40**, 1817 (1989).
[31]J. Wagner, C. Wild, and P. Koidl, Appl. Phys. Lett. **59**, 779 (1991).
[32]J. Birrell, J. E. Gerbi, O. Auciello, J. M. Gibson, D. M. Gruen, and J. A. Carlisle, J. Appl. Phys. **93**, 5606 (2003).
[33]D. M. Gruen, C. D. Zuiker, A. R. Krauss, and X. Pan, J. Vac. Sci. Technol. A **13**, 1628 (1995).
[34]J. Birrell, J. A. Carlisle, O. Auciello, D. M. Gruen, and J. M. Gibson, Appl. Phys. Lett. **81**, 2235 (2002).
[35]T. Katõ, J. Umemura, and T. Takenaka, Mol. Phys. **36**, 621 (1978).